DESIGN OF ENERGY-EFFICIENT ULTRASONIC COMMUNICATION SYSTEMS ON STEEL PIPES

BY

SIJUNG YANG

THESIS

Submitted in partial fulfillment of the requirements
for the degree of Master of Science in Electrical and Computer Engineering
in the Graduate College of the
University of Illinois at Urbana-Champaign, 2017

Urbana, Illinois

Adviser:

Professor Andrew C. Singer

ABSTRACT

Ultrasonic communication provides an alternative to radio-frequency (RF) by transmitting guided ultrasonic signals along installed or buried metallic pipes. Buried pipe corrosion monitoring and intermittent infrastructure data collection are potential application areas, for which reliable wireless links are unavailable due to strong RF attenuation in soil and shielded building infrastructure. When designing a network of such links, energy efficiency, defined as the average energy per transmitted bit, can be far more important than Shannon capacity for such battery-powered, relatively inaccessible links. This work focuses on the low-rate, total life-time energy-limited regime to maximize battery life, while maintaining reliable information transfer at a nominal average rate. The strong frequency selectivity of the through-pipe ultrasonic channel poses several challenges for low-power systems, including strong intersymbol interference (ISI). Previous works have suggested a variety of ad hoc design schemes to implement low-power communication systems satisfying minimum data rate requirements under highly frequency selective and lossy conditions, but failed to propose a systematic methodology to optimize design parameters for energy efficiency. In this work, we apply the concept of energy efficiency maximization to ultrasonic communication over steel pipe channels. A cross-layer approach accounting for both transmit power and signal processing power is suggested, where frequency division multiplexing is explored to counter frequency selectivity. Finally, the bits-per-joule capacity of this channel, based on experimentally measured channel responses, is determined numerically, and an optimized multi-tone frequency shift keying (MFSK) scheme is suggested.

To my parents, for their love and support.

ACKNOWLEDGMENTS

First and foremost, praise and honor to my one and only savior Jesus for all the blessings he permitted me for my entire life.

I would like to express my gratitude to my advisor, Professor Andrew C. Singer, for all the support and patience he showed to me during my master's studies. He always encouraged and helped me find my own academic interests and visions, as well as gave me technical advice when I faced intellectual challenges.

Also, I would like to express my sincerest appreciation to my family back in Korea. They always supported and motivated me by showing their love even thousands of miles away. Without my mother and my father, I could not have been here.

Finally, I want to say thank-you to everyone who directly and indirectly helped me continue my studies, including my friends, teachers, and academic colleagues.

TABLE OF CONTENTS

CHAPTER 1

INTRODUCTION

1.1 Ultrasonic Data Transmission on Infrastructure

Ultrasonic communication has received a lot of attention as an alternative to traditional communication strategies using electric signals. Most notably, underwater wireless acoustic communication technologies have been used for decades as an alternative to electromagnetic transmitting schemes, which have fundamental limits in underwater environments; electromagnetic propagation through water experiences significantly higher attenuation compared to through-air conditions. Several dramatic breakthroughs in throughput maximization of these applications have been also recently reported [1].

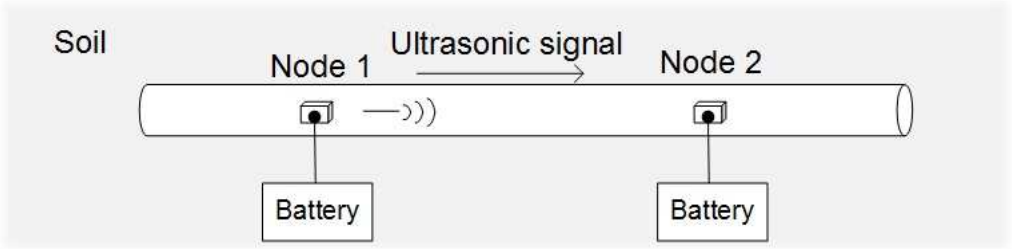

Figure 1.1: Point-to-point communication between pipe health detecting sensors.

Another emerging application is transmission of guided ultrasonic signals through submerged or buried oil, water, or gas pipes, to enable data transfer between remote sensors on the pipes and within the pipe network, as depicted in figure 1.1. In this situation, one of the only practical ways to communicate between sensor nodes is to transmit acoustic signals via steel pipes, because of the strong RF attenuation characteristics of soil and shielded building infrastructure.

1.2 Design Objectives

When designing an ultrasonic communication system using solid-metal guides like pipes, system-level objectives are dramatically different from those traditionally considered when designing wireless RF systems. Energy efficiency is often a more important metric than system throughput; most of its applications target low-rate realization supported only by batteries as shown in figure 1.1. Our goal is to maximize battery life while maintaining reliable information transfer. For instance, assume we want to send 1 kbit of information every day for the system of figure 1.1, supported only by a single AA battery having a capacity of 9000 J. In this case, to achieve more than 10 years of battery life, the average energy consumption per bit sent must be lower than 2.5 mJ.

However, the channel characteristics of pipes pose several challenges when designing such low-power systems. First, metallic pipes are highly lossy media for acoustic propagation. For example, loss is caused by attenuation from acoustic properties of pipes and coupling between the electric transducers and pipes. Second, this channel is highly dispersive with extreme frequency selectivity caused by multi-path propagation; i.e., high levels of intersymbol interference (ISI) appear even at modest bandwidth.

1.3 Preliminary Work

A variety of recent research in acoustic transmission over metal pipes has focused on implementing low-power robust communication systems under highly frequency-selective and lossy conditions. Bacher et al. [2] proposed simple on-off keying (OOK) style modulation with extremely low symbol rates to minimize the complexity of remote water-meter reading systems on steel pipe networks. In [3], multi-tone frequency shift keying (MFSK) was adopted to transmit information through metal enclosures such as shipping containers. To compensate for severe channel dispersion and multi-modality, a time reversal-based pulse position modulation (TR-PPM) method was developed in [4], and a frequency chirp-based OOK scheme was used to realize a low-power ultrasonic communication system through water-filled pipes in

[5]. However, most of these previous works have concentrated on ad hoc low-power implementation of the system rather than optimizing design parameters for energy efficiency in a rigorous manner.

Meanwhile, a number of studies on wireless communication systems [6]-[7] focused on energy-efficient link design, since Verdú defined the concept of capacity per unit cost in his 1990 paper [8]. In [6], it was shown that, in the asymptotic regime, the smallest achievable energy per bit for an additive white Gaussian noise (AWGN) channel is -1.59 dB. Also, maximization of information bits transferred with a given non-asymptotic energy budget was studied in [9]. However, these information-theoretic approaches in [6]-[9] did not consider power additionally consumed by circuit elements during data transmission. A cross-layer approach on power dissipation incorporating both transmitter circuits and RF output was leveraged in [10] to minimize the energy consumption of asymmetric RF microsensor systems. In [11], this cross-layer optimization scheme was adopted to determine optimal transmission time and modulation parameters for energy-efficient communication using M-ary quadrature amplitude modulation (M-QAM) and multiple frequency shift keying (M-FSK) in AWGN channels. These ideas were extended in [7] to energy-efficient link adaptation in frequency-selective channels. This work proposed an energy-efficient water-filling power allocation scheme that adapts both overall power and its allocation based on channel states and circuit power consumption.

1.4 Outline

In this thesis, we provide two synergistic perspectives on the problem of acoustic communication over metal pipes.

- We analyze and model characteristics of the ultrasonic pipe channel based on the underlying physics of the system.
- We extend the concept of energy efficiency maximization into ultrasonic communication along steel pipe channels. A frequency division scheme is adopted to ease ISI induced by frequency selectivity and to realize convenient power allocation for energy efficiency maximization.

In chapter 2, we review the physics of acoustic propagation over a steel pipe system, and suggest a channel model that accounts for such characteristics as high frequency selectivity and amplitude damping. In chapter 3, we formulate the energy efficiency optimization problem for acoustic communication channels described in chapter 2, and provide several practical design examples. Finally, in chapter 4, we conclude and summarize our results.

CHAPTER 2

CHANNEL CHARACTERISTICS OF AN ULTRASONIC PIPE CHANNEL

2.1 Overview

A common metal pipe is a cylindrical shell that can be seen as a solid elastic waveguide to transfer acoustic waves. We can exploit this acousto-mechanical system to send information. A simple model of wireless communication through this type of acoustic waveguide is depicted in figure 2.1.

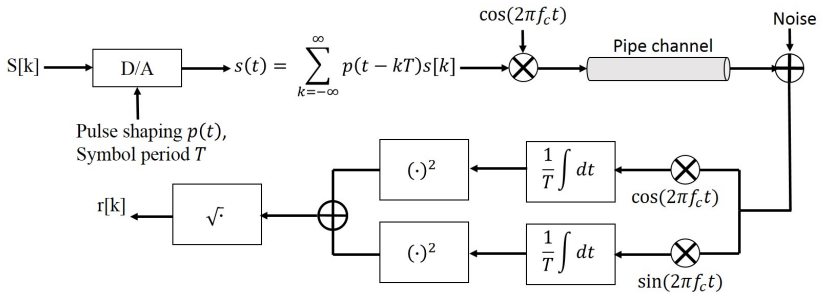

Figure 2.1: An ultrasonic communication scheme through steel pipes using simple on-off keying (OOK) described in [5].

In the system of [5], depicted in figure 2.1, a block of information is encrypted and encoded into binary sequences, and the coded bits are modulated via pulse shaping filters. Then, the passband electric signals translated onto carrier frequencies are driven into attached piezoelectric transducers, resulting mechanical responses which stimulate acoustic propagation axially along the system of steel pipes. We note that, unlike in RF or underwater acoustic communication where spectral properties of transmitting sources or antennas are approximately independent of surrounding materials, piezoelectric transducers' physical characteristics are inherently coupled to some shifts depending on parameters of the pipe system; a pipe itself works as a heavy acoustic impedance to the system when the piezo-transducer is modeled as

an acoustic source. A piezoelectric disc on the receiver side transforms mechanical oscillation into electrical signals. Finally, the acquired waveform passes through demodulation and decoding processes, enabling estimation of the transmitted information sequences.

We next consider the acoustic path between transmitting and receiving transducers to model the channel.

2.2 Ultrasonic Wave Propagation in a Cylindrical Shell

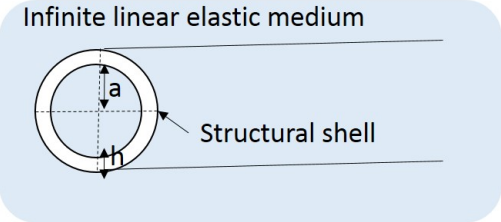

Figure 2.2: A simple model of fluid-filled pipe surrounded by an infinite medium with linear elasticity.

Here, we assume an axially infinite cylindrical shell whose thickness h is less than the radius a of the pipe. Also, as shown in figure 2.2, this pipe is filled with and surrounded by a fluid. Acoustic wave solutions for the given system are derived from the interaction between the solid surface and surrounding fluids. Even though this can be understood as a typical multi-physics problem, it is known that there exists no closed-form solution for general cases [12]. However, for certain conditions like high frequencies and large cylindrical circumferences, this problem can be equivalently unfolded to the infinite plane boundary case like sound propagation along thin plates. More rigorously, when the wavenumber k satisfies $ka >> 1$, the curvature of the surface has little geometric influence on sound radiation. For example, considering a SCH-40 steel pipe 2.54 cm in diameter, we can ignore the geometry of curvature for the frequency ranges well in excess of 31.329 kHz, assuming that the bulk speed of sound on steel is 5000 m/s. Therefore, for ultrasonic communication applications targeting more than hundreds of kHz, the plane boundary approximation can be safely applied. Detailed derivation of solutions to this system can be found in chapter 10 of [12]. Also, acoustic radiation analysis

for lower frequency ranges can be found in [13].

Assume an infinitely extended plane surface surrounded by linear fluid. There exist two different types of waves traveling along the surface: longitudinal (or compressional) and transverse (or shear) waves. If we can ignore viscosity of the fluid, then the traveling longitudinal wave along the plane takes a 2D plane-wave form. Also, it is commonly hard to activate longitudinal waves with transducers attached on the surface, not on the cross-section of a pipe. Therefore, our primary interest will be shear waves, which occur at the surface of the membrane in the form of bending waves. Free-space bending wavenumber k_b is given, for an arbitrary angular frequency ω, by

$$k_b(\omega) = \frac{1}{A}\omega^{1/2}, \tag{2.1}$$

where A denotes a constant related to physical parameters of the elasticity of the plate. For linear fluid surrounding the plane, the acoustic wavenumber k is given by $k = \frac{\omega}{c}$, where c denotes the speed of sound in the fluid. Figure 2.3 shows different dispersion curves for sound waves in fluid and bending waves in a plane boundary.

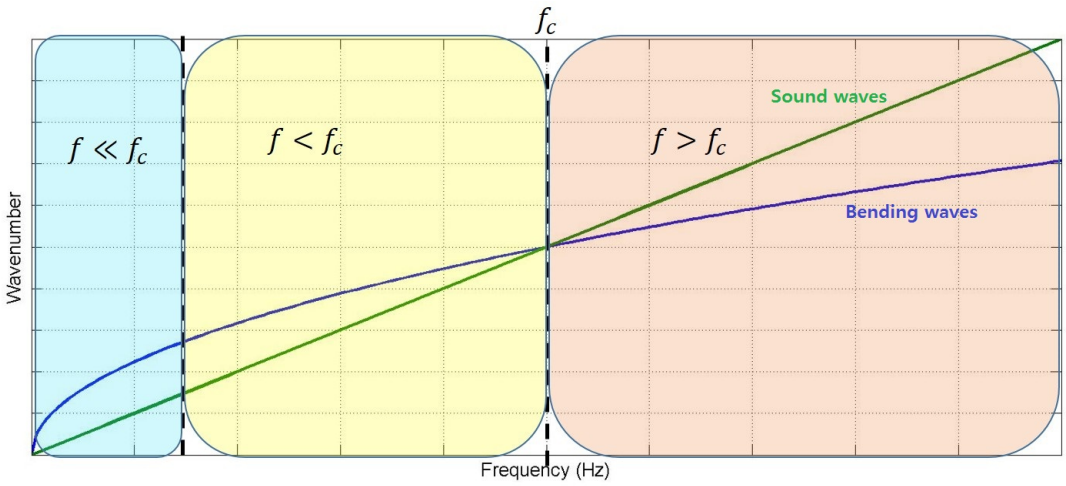

Figure 2.3: Dispersion curves for sound waves and bending waves.

We define f_c, which denotes a frequency where the acoustic wavenumber and the bending wavenumber corresponds to each other, as a *critical frequency*. As can be seen from figure 2.3, we can divide the frequency region into three sections as follows:

1. When $f << f_c$, the speed of bending waves, $v_b = \frac{\omega}{k_b}$ are much lower than the acoustic speed in the fluid. Then, inertial loading by the fluid dominates that by the structural surface, resulting a traveling wave speed independent of the density of the plate, and determined only by the fluid density.

2. When $f < f_c$, inertial loading by the structural plate is comparable to that by the fluid. Therefore, in this case, wave propagation speed is determined by parameters of both surrounding fluid and plate.

3. When $f > f_c$, the speed of membrane waves traveling along the plate exceeds the speed of sound, resulting in nonlinear acoustic propagation typically known as shock waves. In this case, the amplitude of the wave decays exponentially with the travel distance as it loses energy to surrounding fluids.

For a steel plate 0.125 in thick, typical f_c is given in the range between 1 and 10 kHz. Therefore, in the ultrasonic range over hundreds of kHz, where $f >> f_c$, far-field traveling waves from the point source can be written in the following form:

$$s(r, \omega, t) = \frac{1}{r^2} e^{(-\alpha+\beta j)r} e^{j\omega t}, \tag{2.2}$$

where s is vertical displacement, r is traveling distance, ω is angular frequency, β is a wavenumber, and α is an exponential decaying factor.

2.3 Multi-mode Channel Modeling

Figure 2.4 (a) shows that the acoustic communication channel consists of a point source and a point receiver attached on the surface of a pipe. As we have seen in section 2.2, for high enough ultrasonic frequencies, we can ignore geometric effects of the curvature of a pipe. In other words, we can unmap the cylindrical shell coordinates of (a, θ, z) into the equivalent 2D Cartesian coordinates of ($a\theta$, z), as shown in figure 2.4(b).

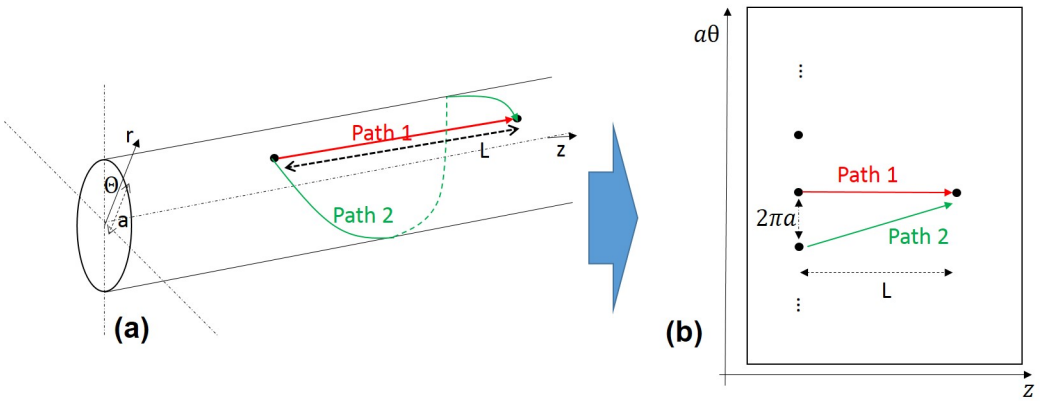

Figure 2.4: (a) Channel paths represented in cylindrical shell coordinates, and (b) its equivalent representation on 2D Cartesian coordinates.

In 2D Cartesian coordinates, a point source in the cylindrical shell is transformed into a spatial array whose aperture length is equivalent to the circumferential length of the pipe. Then the point-source radiation term in (2.1) can be used to construct the acoustic channel model at the point receiver as follows:

$$h_a(\omega) = \frac{1}{L^2} e^{(-\alpha+\beta j)L} + 2\sum_{i=1}^{\infty} \frac{1}{L^2 + 4\pi^2 a^2 i^2} e^{(-\alpha+\beta j)\sqrt{L^2+4\pi^2 a^2 i^2}}. \tag{2.3}$$

Here, L denotes the axial length between the source and the receiver, and β is a wavenumber which is represented in $\frac{\omega}{c}$ by angular frequency ω and the bulk sound of speed c.

Assuming linear coupling, the final electric-to-electric channel model $h(\omega)$ can be computed by multiplying the acoustic channel response of (2.3) by the electro-acoustic response of piezoelectric transducers $h_p(\omega)$, resulting in

$$h(w) = h_a(\omega) h_p(\omega). \tag{2.4}$$

Figure 2.5 shows a simulation result of (2.4) for parameters designated in table 2.1. We can see that there exists high frequency selectivity here, even though we did not assume multi-path from the pipes' routing branches.

Table 2.1: Channel parameters

Axial length	1 m
α (decaying factor)	-0.87 dB/m
speed of shear waves in iron	2000 m/s
diameter of a pipe	0.17m
piezoelectric response	-40dB flat

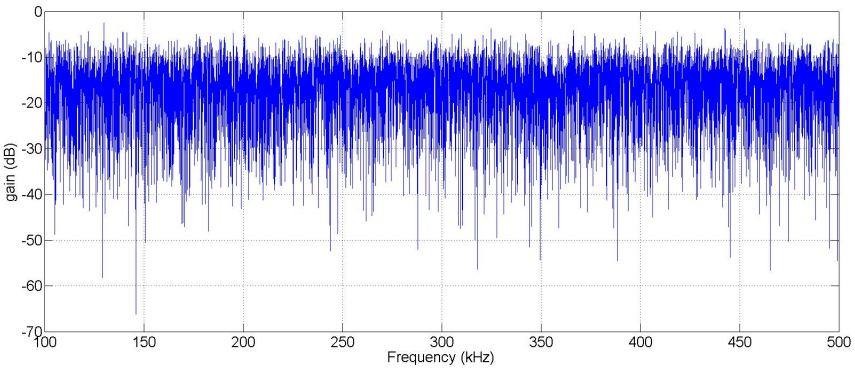

Figure 2.5: Frequency response of the channel based on the model described in (2.4).

2.4 Spectral Measurements of the Channel Response

In this section, channel characteristics of acoustic pipe communication systems based on spectral measurements conducted on steel pipes in a laboratory will be presented.

2.4.1 Experimental Settings

We used SCH-40 galvanized steel pipe 2 m long, with 2.54 cm inside diameter, and 3.175 mm wall thickness. Two piezoelectric (PZT) wafers having dimensions of 10×10×1 mm (PSI-5A4E, Piezo Systems, Inc.) were mounted onto the surface of the pipe with 1 m axial distance to form a bidirectional electric-acoustic channel. Instead of directly attaching transducers to the surface of the pipe, metal rings with clamps were used to enhance acoustic coupling as shown in figure 2.6. Because the pipe is hollow, ultrasonic signals generated by the PZT wafer travel along the pipe's surface. An NI PXI-5421 function generator and an NI PXIe-6368 DAQmx card were used to generate

transmitting signals and sample data from the receiving end. All pre- and post-processing of signals was done in MATLAB.

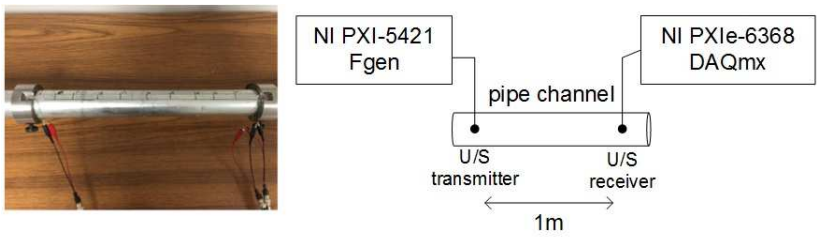

Figure 2.6: Experimental settings of a pipe channel.

2.4.2 Channel Estimation Results

To estimate the channel frequency response, we conducted single-tone measurements from 30 kHz to 500 kHz with a resolution of 10 Hz. Since the observed length of the impulse response τ_{ds} was less than 10 ms, 10 Hz $\ll$ 100 Hz resolution was sufficiently fine. The measured magnitude response of this channel in frequency domain is shown in figure 2.7. We can observe that this channel has multiple resonance peaks induced not only by the PZT transducer, which has only two resonance peaks at 100 kHz, and 250 kHz, but also by the multi-mode acoustic properties of the steel pipe, depicted in the previous section and coupling behavior between them.

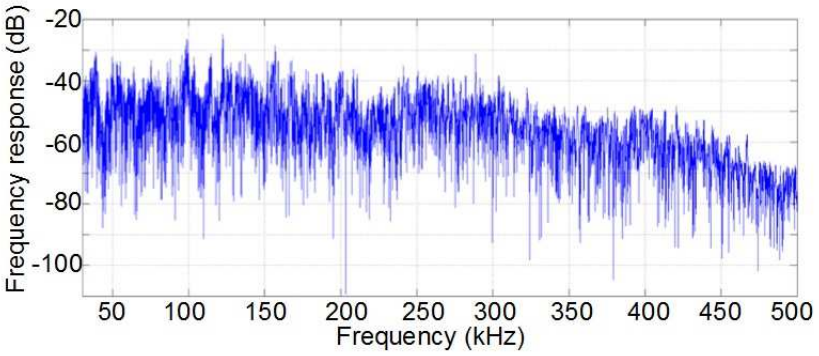

Figure 2.7: Experimental voltage transfer function of the channel described in figure 2.6.

CHAPTER 3

ENERGY EFFICIENCY OPTIMIZATION

3.1 Energy-Efficient Communication over AWGN Channels

In this section, an energy efficiency optimization problem for point-to-point communication over AWGN channels will be briefly reviewed, where, for now, we ignore the frequency selectivity of the pipe channel.

Assume an AWGN channel with noise density N_0 and available frequency bandwidth W. We send K bits through this channel at an average rate R using a total of E joules of over a time period of ΔT. Then, U, the *energy efficiency*, can be defined as

$$U \triangleq \frac{K}{E} = \frac{R\Delta T}{P\Delta T} = \frac{R}{P}, \tag{3.1}$$

where P refers to the average power consumption from transmitting the signals. From Shannon's capacity formula, the maximum achievable rate with a given transmit power P is given by

$$C = W \log_2(1 + \frac{P}{WN_0}). \tag{3.2}$$

Now, *bits-per-joule capacity* C_e, which is defined in [8] as the maximum information that can be sent with arbitrarily low probability of error using a unit amount of energy, can be computed by maximizing U over P, assuming capacity-achieving transmission, i.e.,

$$C_e = \sup_{P>0} \frac{R}{P} = \sup_{P>0} \frac{W \log_2(1 + \frac{P}{WN_0})}{P} = \frac{1}{N_0 \ln 2}. \tag{3.3}$$

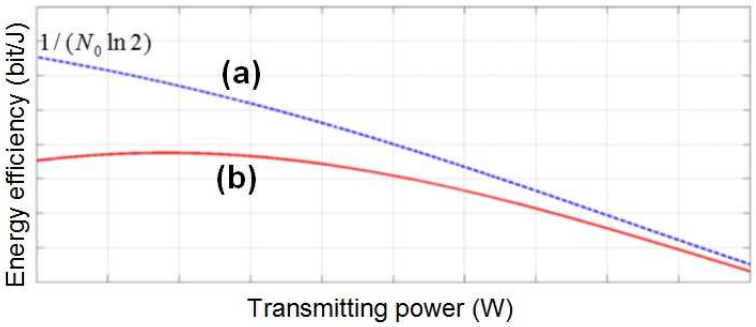

Figure 3.1: Energy efficiency curve in terms of transmit power, where circuit power term is (a) not included, and (b) included.

As shown in figure 3.1, bits-per-joule capacity C_e is achieved when the transmitting power consumption P approaches zero. It is interesting to compare how Shannon capacity and energy efficiency change with transmitting power. As can be seen from figure 3.1 (a), energy efficiency is a monotonically decreasing function of transmitting power, while traditional Shannon capacity is monotonically increasing with power consumption. This gives a simple but important intuition on design for energy-efficient communication systems: for energy efficiency maximization, system design must be done within a low-power and low-rate regime. Note that so far we only considered transmitted symbol power to compute energy efficiency.

In common wireless systems communicating between long distances at high data rates, it is assumed that the power consumed by signal processing is low compared to the power spent generating the transmitted waveform. However, in an energy efficiency maximizing setting, we know from our previous discussion that a low-rate and low-power scheme is adopted, and this means that total power must include a circuit power term for accurate representation of energy efficiency.

Generally, in a wireless system with fixed frequency bandwidth, circuit power can be simply modeled as a constant term P_c independent of data rate [10]. In practice, this term includes energy consumption of all devices of the circuit except those like amplifier modules, whose power spending is proportional to the transmit power. We can include this term in U. Then, energy efficiency can be rewritten as $U = \frac{R}{P_c+P}$. Bits-per-joule capacity is then given by [7]

$$C_e = \sup_{P>0} \frac{W \log_2(1 + \frac{P}{WN_0})}{P + P_c}, \tag{3.4}$$

and the maximizing $P = P^*$ for C_e satisfies the following equation:

$$\log_2(1 + \frac{P^*}{WN_0}) = \frac{P^* + P_c}{(N_0W + P^*)\ln 2}. \tag{3.5}$$

As can be seen from figure 3.1 (b), introduction of circuit power breaks the monotonic relation between power and energy efficiency, and transforms the curve such that the optimal point where the energy efficiency is maximized is more away from $P = 0$. Note that the energy optimization methodology described in this section can be applied not only to derive theoretical bounds, but also to design practical systems. For example, if an uncoded M-ary PSK scheme is adopted in this AWGN communication channel, then the bit error probability is approximated as [14]

$$P_b \approx \frac{2}{k} e^{-\frac{P}{N_0W} sin^2 \frac{\pi}{2^k}}, \tag{3.6}$$

where k is the modulation number of M-ary PSK, i.e. $k = \log_2 M$. We can derive the required transmit power for a given P_b in terms of modulation number from (3.6):

$$P \approx \frac{N_0W \ln \frac{2}{kP_b}}{\sin^2 \frac{\pi}{2^k}}. \tag{3.7}$$

Also, the data rate R is given by $R \approx kW$. Therefore, we can optimize energy efficiency in terms of the modulation number by solving

$$\sup_{k\in\mathbb{N}} U = \sup_{k\in\mathbb{N}} \frac{kW}{P_c + \frac{N_0W \ln \frac{2}{kP_b}}{sin^2 \frac{\pi}{2^k}}}. \tag{3.8}$$

Note that the denominator of the right-hand side is a convex function, so this problem can be easily solved by the gradient assisted binary search (GABS) algorithms [7].

3.2 Energy-Efficient Communication over an Acoustic Channel using Steel Pipes

In the following section, we will present a methodology to optimize energy efficiency in highly frequency-selective channels like the one described in sec-

tion 3.1. To counter the high level of ISI introduced by frequency selectivity, families of frequency division modulation schemes can be used: instead of sending a wide-band signal over a single frequency-selective channel, information is sent over multiple narrow, but flat response subchannels. One apparent advantage of this scheme is that it naturally diminishes ISI in each subchannel, potentially simplifying the equalization process. More importantly, by dividing a wide band into a number of subchannels, we have more degrees of freedom over which to allocate power over the frequency domain to maximize energy efficiency. Note that frequency division can be easily implemented with low complexity structures, using well known schemes such as orthogonal frequency division modulation (OFDM).

Assume the entire bandwidth is divided into $K \gg 1$ subchannels each of which has a bandwidth of B. Note that B is arbitrarily chosen with $B \ll \frac{1}{\tau_{ds}}$ to guarantee each subchannel has approximately flat gain. Denote noise spectral density as N_0, the power gain of the i^{th} subchannel as g_i, and the allocated transmit power on the i^{th} subchannel as P_{T_i}. We send data through the i^{th} subchannel with the data rate r_i, and the data rates on each subchannel form a data rate vector $\boldsymbol{R} = [r_1, r_2, ..., r_K]^T$. The overall data rate R is represented by the sum of r_i's, i.e., $R = \sum_{i=1}^{K} r_i$.

Now, we can obtain a representation for energy efficiency by using similar approaches to those in chapter 2. Denote total power consumption as P_{total} provided as follows:

$$P_{total} = P_C(\boldsymbol{R}) + \sum_{i=1}^{K} P_{T_i}(r_i), \tag{3.9}$$

where $P_C(\boldsymbol{R})$ refers to a circuit power function of the data rate vector $\boldsymbol{R}$. Accordingly, energy efficiency U is represented by a function of the data rate vector $\boldsymbol{R}$ as follows:

$$U(\boldsymbol{R}) = \frac{\sum_{i=1}^{K} r_i}{P_C(\boldsymbol{R}) + \sum_{i=1}^{K} P_{T_i}(r_i)}. \tag{3.10}$$

Assuming this channel adopts encoding and modulation schemes which achieve Shannon capacity, then, r_i is given by $r_i = B\log_2(1 + \frac{P_{T_i} g_i}{N_0 B})$, and

$$\sum_{i=1}^{K} P_{T_i}(r_i) = \sum_{i=1}^{K} (2^{r_i/B} - 1)\frac{N_0 B}{g_i}. \tag{3.11}$$

Note that transmit power on each subchannel P_{T_i} can be modeled differently by various modulation and encoding schemes. For example, for uncoded M-PSK, P_{T_i} can be represented by (3.7).

In the wireless link adaptation problems described in [10] and [7], it is shown that circuit power can be simply modeled as a constant independent of transmission rates. Therefore, in this regime, our optimization problem can be written to find an optimal $\boldsymbol{R} = \boldsymbol{R}^*$ which maximizes $U(\boldsymbol{R})$ as follows:

$$\boldsymbol{R}^* = \arg\max_{\boldsymbol{R}\succeq\boldsymbol{0}} \frac{\sum_{i=1}^{K} r_i}{P_C + \sum_{i=1}^{K} (e^{r_i/B} - 1)\frac{N_0 B}{g_i}}. \tag{3.12}$$

It is known [7] that, as long as the denominator on the right-hand side of (3.12) is a convex function of $\boldsymbol{R}$, a unique global optimum solution exists, and families of gradient descent algorithms can be used to obtain numerical results. In fact, the solution $\boldsymbol{R}^*$ to (3.12) satisfies following relation:

$$P_{T_i} = \left[\frac{B}{U(\boldsymbol{R}^*)} - \frac{N_0 B}{g_i}\right]^+, \tag{3.13}$$

which can be interpreted as a solution to a water-filling problem with a total power constraint of $\sum_{i=1}^{K} P_{T_i}$. Note that we are utilizing only subchannels having gains larger than $U(\boldsymbol{R}^*)N_0$ in this case. For the following discussion, I will use the term *utilized subchannels* to denote subchannels with $P_{T_i} > 0$, or $r_i > 0$.

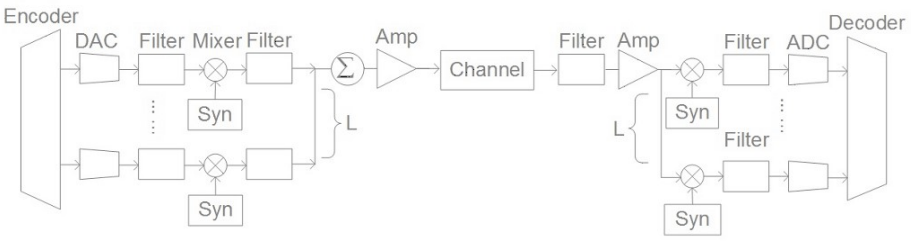

Figure 3.2: Block diagram of a typical frequency division modulation scheme, but not an OFDM system.

However, in our application, it is no longer valid to assume circuit power is independent of $\boldsymbol{R}$. More precisely, the circuit power of our system is determined by the range of utilized subchannels, i.e., the circuit power consumption depends only on whether $r_i > 0$ or $r_i = 0$. In an RF wireless system, because of strict constraints on frequency bandwidth, the circuit system can be designed to utilize all subchannels located in the available frequency range, and must be designed so that the system can deal with a time-fading property. Therefore, the circuit power of the RF system is predetermined by the bandwidth constraint, and independent of energy-efficient link adaptation. Meanwhile, there is no hard constraint on choosing frequency bandwidth in ultrasonic communication; i.e., a bandwidth is considered to be a design parameter, not a fixed constraint. Therefore, the power consumption structures of a circuit are also changing with it. For instance, if we assume circuit power is constant independent of bandwidth, then we reach the conclusion that a system utilizing infinite bandwidth maximizes energy efficiency, which is invalid in practical applications.

Modeling circuit power as a function of data rate is generally an open-ended problem. Therefore, in order to narrow our scope to specific design schemes, we suggest two kinds of systems. Figure 3.2 is a block diagram of a traditional frequency division modulation scheme. In this scheme, the modulation/demodulation process of each subchannel is operated separately in each subsystem. Assume L out of K subchannels are chosen to be utilized. Then, circuit power P_C, which is not linearly proportional to transmit power, can be modeled as follows:

$$P_C \approx P_D + L(P_{flt} + P_{syn} + P_{mix} + P_{ADC} + P_{DAC}), \tag{3.14}$$

where P_D, P_{flt}, P_{syn}, P_{mix}, P_{ADC}, and P_{DAC} are values of power consumed by digital domain processing, active filters, frequency synthesizers, mixers, analog-to-discrete converters (ADC), and discrete-to-analog converters (DAC) during transmission time in each subsystem. Denoting $P_A = P_{flt} + P_{syn} + P_{ADC} + P_{DAC}$, we can apply this model to (3.10) as follows:

$$U(\boldsymbol{R}) = \frac{\sum_{i=1}^{K} r_i}{P_D + P_A\|\boldsymbol{R}\|_0 + \sum_{i=1}^{K} P_{T_i}(r_i)}, \tag{3.15}$$

where $\|\boldsymbol{R}\|_0$, the l_0-norm of the data rate vector $\boldsymbol{R}$, is equal to L.

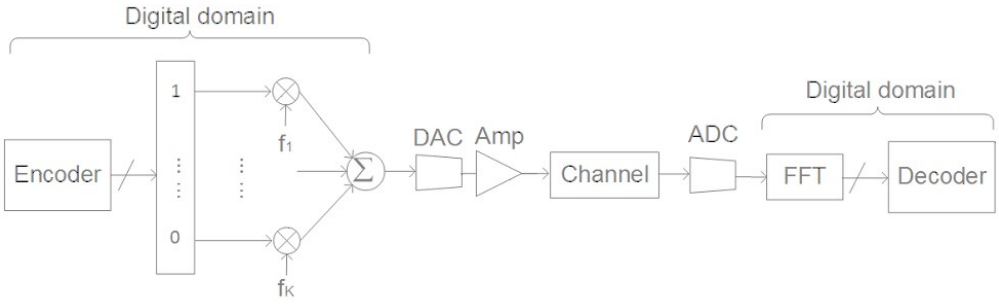

Figure 3.3: MFSK communication scheme suggested in [3].

We can also think of a system where most signal generation is conducted in the digital domain. A typical example is shown in figure 3.3, which describes the multi-tone FSK (MFSK) system for ultrasonic communication along metal surfaces suggested in [3]. Instead of using analog filters and mixers to separate signals in different subchannels as in figure 3.2, all of the separation process is done in discrete time, using a single DAC and ADC to translate the signal between digital and analog. The circuit power consumption model for this system can be provided by the following:

$$P_C \approx P_D + P_{ADC} + P_{DAC}. \tag{3.16}$$

As illustrated in [11], $P_{ADC} \approx \alpha f_s$, and $P_{DAC} \approx \beta + \gamma f_s$, where α, β, and γ are constant coefficients, and f_s is the sampling frequency. By leveraging a principle of bandpass sampling, f_s can be minimized as $f_s \approx 2B_0$ without aliasing, where B_0 is an intermediate frequency (IF) bandwidth of the signal. More precisely, $f_s = 2(2B+f_{cor})$ is often used, where f_{cor} is a corner frequency of the $1/f$ noise in the ADC. Denote the largest carrier frequency among those of utilized subchannels by f_{max}, and the smallest one by f_{min}. Then, IF bandwidth B_0 can be represented as $B_0 = f_{max} - f_{min} + 2B$. By summing up all of these terms, we derive a power consumption model in terms of f_{max} and f_{min}, i.e., $P_C = C + D(f_{max} - f_{min})$, where C and D are technology-specific constants. Applying this to (3.10) yields

$$U(\boldsymbol{R}) = \frac{\sum_{i=1}^{K} r_i}{C + D(f_{max} - f_{min}) + \sum_{i=1}^{K} P_{T_i}(r_i)}. \tag{3.17}$$

Maximization of (3.15) and (3.17) can be interpreted as a mixed integer programming problem which has a mixed structure of combinatorial and convex optimizations. For example, maximization of (3.15) can be written as

$$\begin{aligned} U(\boldsymbol{R}^*) &= \max_{\boldsymbol{R}\succeq\mathbf{0}} \frac{\sum_{i=1}^{K} r_i}{P_D + P_A\|\boldsymbol{R}\|_0 + \sum_{i=1}^{K} P_{T_i}(r_i)} \\ &= \max_{s\in\boldsymbol{S}} \max_{\boldsymbol{R}\succeq\mathbf{0}, S(\boldsymbol{R})=s} \frac{\sum_{i=1}^{K} r_i}{P_D + P_A\Gamma(s) + \sum_{i=1}^{K} P_{T_i}(r_i)}. \end{aligned} \tag{3.18}$$

If we fix the support of data rate vector $S(\boldsymbol{R})$ to a support s, then $\|\boldsymbol{R}\|_0$ is also fixed to a constant value $\Gamma(s)$. Then, this problem is analogous to the constant circuit power case as described in (3.12), and can be solved as a convex optimization problem for each s. Since the cardinality of the set of all supports $\boldsymbol{S}$ is finite, the rest of procedure is equal to combinatorial optimization problems on $\boldsymbol{S}$. Because the cardinality of $\boldsymbol{S}$ is 2^K, the complexity of this combinatorial problem seems to be $O(2^K)$. However, in fact, we can reduce the complexity down to $O(K)$ by cleverly choosing supports to maximize channel gains. From the set of supports s.t. $\|\boldsymbol{R}\|_0 = \Gamma(s)$, we know by intuition that the best support to maximize energy efficiency is the support that includes the Γ subchannels with highest gains.

3.3 Design Examples: Uncoded and Coded MFSK

One typical example which uses the architecture illustrated in figure 3.2 is a frequency shift keying (FSK) modulation scheme. *Multi-tone FSK* (MFSK) is a more general variation of the traditional FSK in that it utilizes multiple frequencies, instead of a single-tone, to construct a symbol. Like other orthogonal modulation schemes, MFSK also satisfies the asymptotically capacity-achieving property in the wide-band limit, while it allows lower peak power per tone than traditional FSK [15]. In [3], this property of MFSK was leveraged to implement low-power data communication using ultrasonic signals through metallic guides. In this section, we suggest a well formulated method based on the energy efficiency optimization problem described in (3.18) to determine design parameters of an MFSK structure.

3.3.1 Uncoded MFSK

Denote the total number of utilized tones by M. Note that we automatically choose tones with M highest channel gains. Then, the uncoded-MFSK scheme, where each of all possible 2^M symbols has equal *prior*, is equivalent to the set of M parallel on-off keying (OOK) channels with different channel gains g_i's. For the coherent case, the bit error probability of the each i^{th} tone is given as [16]

$$P_{e,i} = \frac{1}{2}\text{erfc}\left(\sqrt{\frac{P_{T_i}g_i}{4N_0B}}\right) \leq \frac{1}{2}e^{-\frac{P_{T_i}g_i}{4N_0B}}. \tag{3.19}$$

If we denote the average BER requirement as P_e, we can write a bound on the system constraint with the fixed M as

$$\frac{1}{M}\sum_{i=1}^{M}\frac{1}{2}e^{-\frac{P_{T_i}g_i}{4N_0B}} \leq P_e. \tag{3.20}$$

In addition, energy efficiency can be represented as the following:

$$U(\boldsymbol{P_T}) = \frac{M}{P_D + P_A M + \sum_{i=1}^{M} P_{T_i}}, \tag{3.21}$$

where $\boldsymbol{P_T}$ is the vector of the transmit power. Therefore, for the fixed M, maximization of $U(\boldsymbol{P_T})$ is equivalent to minimization of $\sum_{i=1}^{K} P_{T_i}$ with respect to (3.20). Because this satisfies KKT conditions, we can use the method of Lagrange multipliers to solve the problem as the following:

$$\nabla\left(\sum_{i=1}^{M} P_{T_i}\right) + \lambda\nabla\left(\frac{1}{M}\sum_{i=1}^{M}\frac{1}{2}e^{-\frac{P_{T_i}g_i}{4N_0B}} - P_e\right) = 0. \tag{3.22}$$

Then,

$$P_{T_i} = \frac{4N_0B}{g_i}\ln\frac{\mu g_i}{2MP_e}, \tag{3.23}$$

where $\mu = \sum_{i=1}^{M}\frac{1}{g_i}$. Accordingly, energy efficiency U is solely determined by the total number of tones M, and maximizing M can be obtained by exhaustive search:

$$M = \arg\max_{M\in\mathbb{Z}^+} \frac{M}{P_D + P_A M + \sum_{i=1}^{M}\frac{4N_0B}{g_i}\ln\frac{\mu g_i}{2MP_e}}. \tag{3.24}$$

3.3.2 Coded MFSK

The maximum achievable rate of coded MFSK can be derived similarly to the uncoded case by treating this scheme as K parallel OOK channels. If we adopt hard-decision decoding, then each OOK channel is equivalent to the binary symmetric channel with the error probability $\epsilon_i \leq \frac{1}{2}e^{-\frac{P_{T_i}g_i}{4N_0B}}$. Therefore, the capacity of the entire channel can be represented in terms of the transmit power vector $\boldsymbol{P_T}$ as the following:

$$C = \sum_{i=1}^{K} 1 - H_2(\epsilon_i), \tag{3.25}$$

where $H_2(\cdot)$ is the binary entropy function. Therefore, the energy efficiency optimization problem can be expressed as the following:

$$\boldsymbol{P_T} = \arg\max_{\boldsymbol{P_T} \succeq \boldsymbol{0}} \frac{\sum_{i=1}^{K} 1 - H_2(\epsilon_i)}{P_{code} + P_D + P_A\|\boldsymbol{P_T}\|_0 + \sum_{i=1}^{K} P_{T_i}}, \tag{3.26}$$

where P_{code} represents the additionally consumed power used by the coding and decoding process.

3.3.3 Numerical Results

Table 3.1: System parameters

Number of subchannels	4700
Bandwidth of each subchannel	100 Hz
Thermal noise power, N_0	-90 dBW/Hz
Circuit power model, $P_D + P_A\|\boldsymbol{R}\|_0$	P_D=1 mW, P_A=0.5 mW
Channel	1 m length cylindrical pipe channel
Bit error rate	$\leq$ 1E-06

In this section, numerical solutions to (3.18), (3.24), and (3.26) are presented with system parameters stated in table 3.1. The binary search assisted ascent (BSAA) algorithm presented in [7] is used to solve the convex optimization part of the mixed integer programming problem (3.18). Note that we used an actual channel response of the pipe channel illustrated in section 2.4.

If we assume a virtual scheme that achieves Shannon capacity as in (3.13), the optimal energy efficiency solution that we obtain here can be interpreted as the bits-per-joule capacity of this pipe channel. As shown in figure 3.4, a maximum energy efficiency of 522.85 kbit/J is achieved when $\Gamma = 19$ sub-channels are utilized. The corresponding total data rate and total power consumption are 7.3494 kb/s and 14.1 mW.

Figure 3.5 shows energy efficiency graphs of coded and uncoded MFSK schemes. As can be seen, at optimal number of tones $M^* = 17$, energy efficiency is maximized to 1.3068 kbit/J for the uncoded case. If we ignore the power consumed by coding process P_{code}, maximum energy efficiency is approximately 1.3996 kbit/J which results in 8% gain in terms of energy efficiency. However, if 1 mW of computing power is spent on coding process, then the gain is reduced to 3%. Furthermore, if more than 1.7mW of computing power is required on the coding, we are unable to enhance energy efficiency by coding.

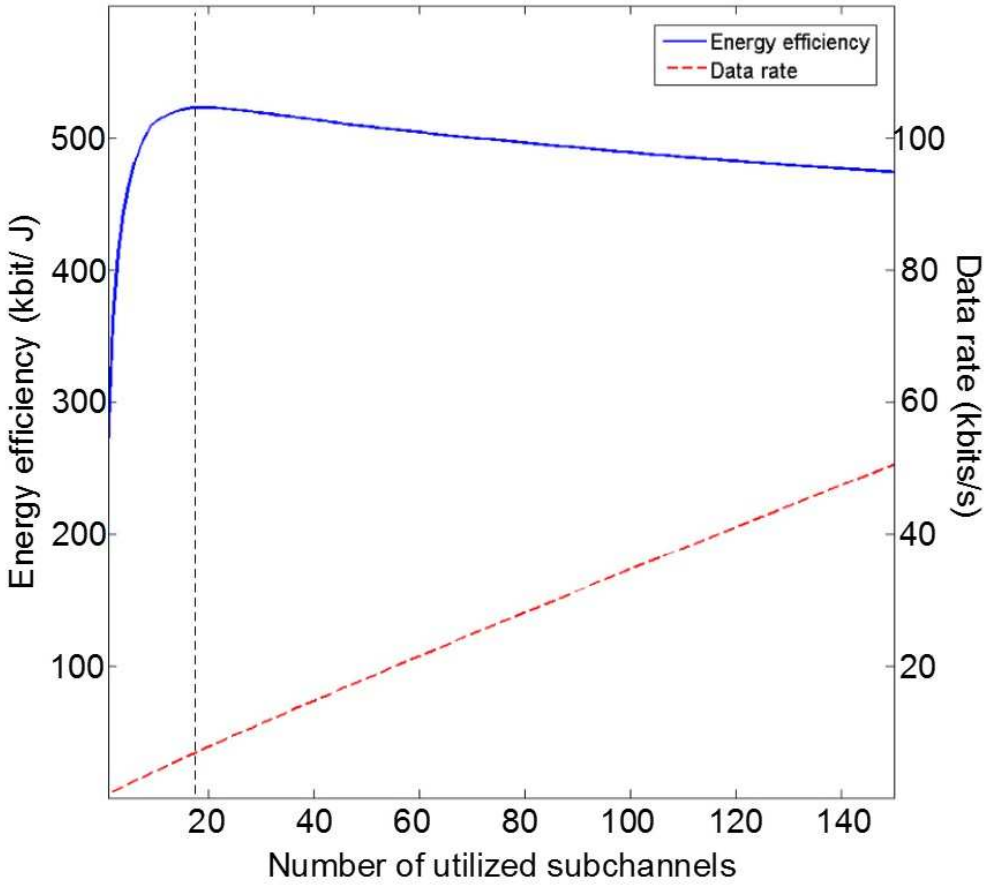

Figure 3.4: Maximum achievable energy efficiency with respect to the number of utilized subchannels.

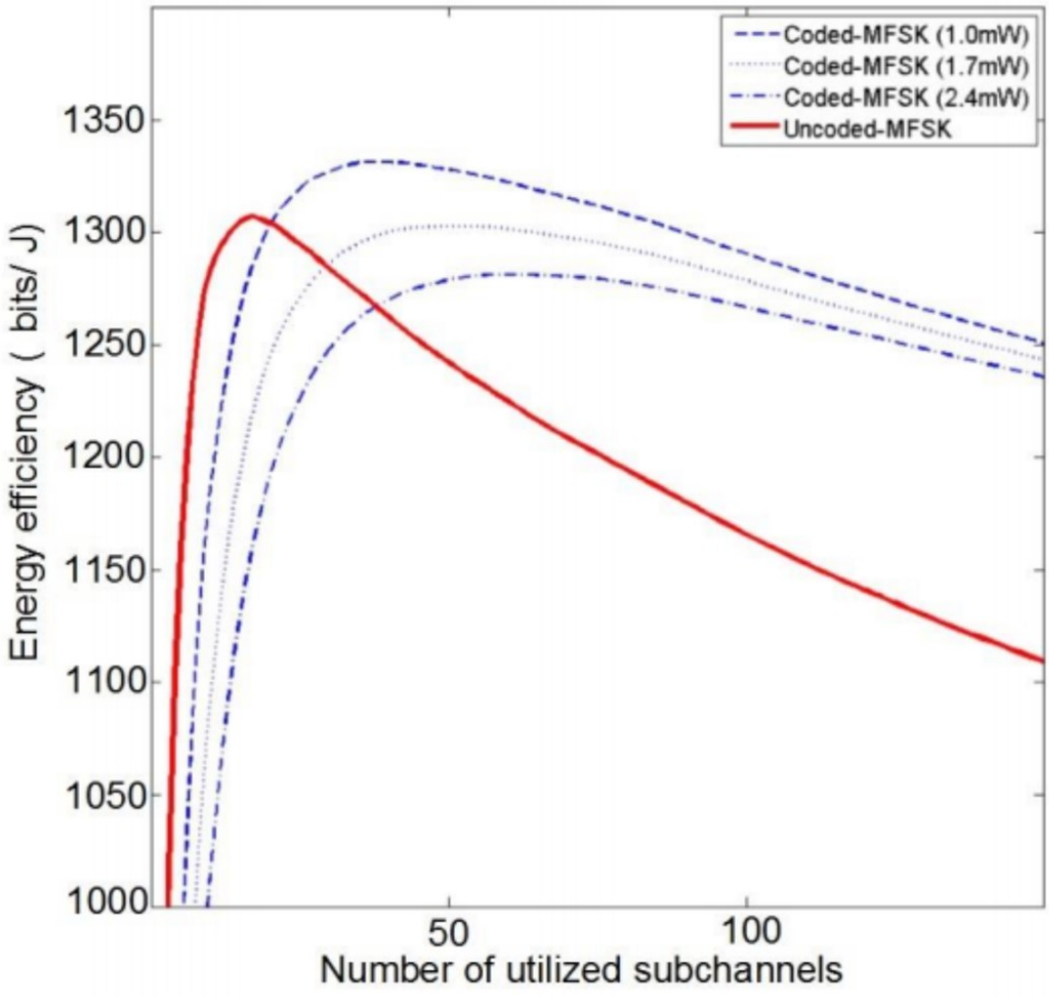

Figure 3.5: Energy efficiency of coded and uncoded MFSK schemes.

CHAPTER 4

CONCLUSION

In this work, we investigated various perspectives of the interesting technical problem of ultrasonic communication along steel pipe networks.

First, we reviewed and summarized acoustic and mechanical properties of wave propagation in a fluid-loaded cylindrical shell at ultrasonic frequencies. Based on the observation, we successfully suggested a model which can account for the frequency selectivity and attenuation properties of the channel.

We then extended a concept of energy efficiency optimization for a communication system into the field of ultrasonic communication along solid metal guides. To counter the frequency selectivity of pipe channels, we suggested a frequency division modulation structure. In addition, based on the frequency division frameworks, we mathematically formulated the energy efficiency optimization problem of the ultrasonic communication system over pipes. This was achieved by a cross-layer approach accounting for both transmit power and signal processing power. Finally, the proof of concept was given in examples of the system using a multi-tone frequency shift keying (MFSK) scheme.

REFERENCES

[1] T. Riedl and A. Singer, "Towards a video-capable wireless underwater modem: Doppler tolerant broadband acoustic communication," in *Underwater Communications and Networking (UComms), 2014*. IEEE, 2014, pp. 1–5.

[2] C. Bacher, P. Palensky, and S. Mahlknecht, "Low cost data transmission via metallic solids for sensor networking," in *Emerging Technologies, 2005. Proceedings of the IEEE Symposium on*, Sept 2005, pp. 193–198.

[3] T. Hosman, M. Yeary, J. K. Antonio, and B. Hobbs, "Multi-tone FSK for ultrasonic communication," in *Instrumentation and Measurement Technology Conference (I2MTC), 2010 IEEE*, May 2010, pp. 1424–1429.

[4] Y. Jin, Y. Ying, and D. Zhao, "Data communications using guided elastic waves by time reversal pulse position modulation: Experimental study," *Sensors*, vol. 13, no. 7, p. 8352, 2013. [Online]. Available: http://www.mdpi.com/1424-8220/13/7/8352

[5] S. Chakraborty, G. J. Saulnier, K. W. Wilt, R. B. Litman, and H. A. Scarton, "Low-rate ultrasonic communication axially along a cylindrical pipe," in *Ultrasonics Symposium (IUS), 2014 IEEE International*, Sept 2014, pp. 547–551.

[6] S. Verdú, "Spectral efficiency in the wideband regime," *IEEE Transactions on Information Theory*, vol. 48, no. 6, pp. 1319–1343, Jun 2002.

[7] G. Miao, N. Himayat, and G. Y. Li, "Energy-efficient link adaptation in frequency-selective channels," *IEEE Transactions on Communications*, vol. 58, no. 2, pp. 545–554, February 2010.

[8] S. Verdú, "On channel capacity per unit cost," *IEEE Transactions on Information Theory*, vol. 36, no. 5, pp. 1019–1030, Sept 1990.

[9] Y. Polyanskiy, H. V. Poor, and S. Verdu, "Minimum energy to send k bits through the Gaussian channel with and without feedback," *IEEE Transactions on Information Theory*, vol. 57, no. 8, pp. 4880–4902, Aug 2011.

[10] A. Y. Wang, S. Cho, C. G. Sodini, and A. P. Chandrakasan, "Energy efficient modulation and MAC for asymmetric RF microsensor systems," in *Low Power Electronics and Design, International Symposium on, 2001.*, 2001, pp. 106–111.

[11] S. Cui, A. J. Goldsmith, and A. Bahai, "Energy-constrained modulation optimization," *IEEE Transactions on Wireless Communications*, vol. 4, no. 5, pp. 2349–2360, Sept 2005.

[12] M. J. Crocker, *Handbook of Acoustics*. John Wiley & Sons, 1998.

[13] J. M. Muggleton, M. Brennan, and R. Pinnington, "Wavenumber prediction of waves in buried pipes for water leak detection," *Journal of Sound and Vibration*, vol. 249, no. 5, pp. 939–954, 2002.

[14] J. G. Proakis, *Digital Communications*. New York: McGraw-Hill, 2000.

[15] C. Luo, M. Medard, and L. Zheng, "On approaching wideband capacity using multitone FSK," *IEEE Journal on Selected Areas in Communications*, vol. 23, no. 9, pp. 1830–1838, Sept 2005.

[16] Q. Tang, S. K. S. Gupta, and L. Schwiebert, "Ber performance analysis of an on-off keying based minimum energy coding for energy constrained wireless sensor applications," in *IEEE International Conference on Communications, 2005. ICC 2005. 2005*, vol. 4, May 2005, pp. 2734–2738.